JOURNAL OF AGRICULTURAL AND FOOD CHEMISTRY

Enzymatic Synthesis of a Selective Inhibitor for α-Glucosidases: α-Acarviosinyl-(1→9)-3-α-D-glucopyranosylpropen

YOUNG-SU LEE,[†] MYOUNG-HEE LEE,[†] HEE-SEOB LEE,[‡] SEUNG-JAE LEE,[†] YOUNG-WAN KIM,[§] RAN ZHANG,[||] STEPHEN G. WITHERS,[||] KWAN SOO KIM,[⊥] SUNG-JOON LEE,[#] AND KWAN-HWA PARK*,[†]

Center for Agricultural Biomaterials and School of Agriculture and Biotechnology, Seoul National University, Seoul 151-921, Korea, Department of Food and Nutrition, Pusan National University, Pusan 609-735, Korea, Department of Food and Biotechnology, Korea University, Jochiwon 339-700, Korea, Department of Chemistry, University of British Columbia, Vancouver, BC V6T 1Z4, Canada, Department of Chemistry, College of Science, Yonsei University, Seoul 120-749, Korea, and Division of Food Bioscience and Technology, Korea University, Seoul 136-713, Korea

Here, we describe the enzymatic synthesis of novel inhibitors using acarviosine-glucose as a donor and 3-α-D-glucopyranosylpropen (αGP) as an acceptor. Maltogenic amylase from *Thermus* sp. (ThMA) catalyzed the transglycosylation of the acarviosine moiety to αGP. The two major reaction products were isolated using chromatographies. Structural analyses revealed that acarviosine was transferred to either C-7 or C-9 of the αGP, which correspond to C-4 and C-6 of glucose. Both inhibited rat intestine α-glucosidase competitively but displayed a mixed-type inhibition mode against human pancreatic α-amylase. The α-acarviosinyl-(1→7)-3-α-D-glucopyranosylpropen showed weaker inhibition potency than acarbose against both α-glycosidases. In contrast, the α-acarviosinyl-(1→9)-3-α-D-glucopyranosylpropen exhibited a 3.0-fold improved inhibition potency against rat intestine α-glucosidase with 0.3-fold inhibition potency against human pancreatic α-amylase relative to acarbose. In conclusion, α-acarviosinyl-(1→9)-3-α-D-glucopyranosylpropen is a novel α-glucosidase-selective inhibitor with 10-fold enhanced selectivity toward α-glucosidase over α-amylase relative to acarbose, and it could be applied as a potent hypoglycemic agent.

KEYWORDS: Maltogenic amylase from *Thermus* sp.; acarbose; 3-α-D-glucopyranosylpropen; inhibitor; transglycosylation

INTRODUCTION

The development of α-glycosidase inhibitors is of particular interest because of their therapeutic potential in the management of diabetes (*1–3*). Selective inhibition against α-glucosidases over α-amylases is important to allow polysaccharides in the diet to be hydrolyzed by α-amylases, after which absorption of the resulting oligosaccharides in the small intestine follows (*4*). If undigested polysaccharides enter the colon because of the strong inhibition of α-amylases by drugs, side effects including flatulence are possible as a consequence of bacterial fermentation (*4*).

Acarbose, a pseudotetrasaccharide, consists of acarviosine and maltose, which are linked via an α-(1→4)-glycosidic linkage (**Figure 1**), and is a well-known as a potent inhibitor of α-glycosidases (*5, 6*). Although acarbose is widely used as a therapeutic agent for diabetes (*7, 8*), its inhibition mechanism is somewhat obscure. In several three-dimensional structures of different α-amylases cocrystallized with acarbose, a substantially rearranged product, pseudopentasaccharide, was found in the subsites −3 through +2 (*9, 12*). The enzymatic modification of acarbose presumably occurs as a result of a series of enzymatic hydrolysis, condensation, and transglycosylation events (*13*). Given these enzymatic modifications of acarbose, there have been several attempts to synthesize elongated acarbose derivatives as strong inhibitors through *in situ* extension using an α-amylase (*14, 15*).

Maltogenic amylases (MAases) are members of the glycoside hydrolase family 13, which not only hydrolyzes cylcodextrins, starch, and pullulan but also catalyzes transglycosylation to form α-(1→6)-glycosidic linkages as well as α-(1→4)-linkages (*16*). In addition, MAases can hydrolyze acarbose to acarviosine-

* Corresponding author. Tel: 82-2-8804852. Fax: 82-2-8735095. E-mail: parkkh@snu.ac.kr.
[†] Seoul National University.
[‡] Pusan National University.
[§] Department of Food and Biotechnology, Korea University.
[||] University of British Columbia.
[⊥] Yonsei University.
[#] Division of Food Bioscience and Technology, Korea University.

10.1021/jf703655k CCC: $40.75
Published on Web 06/14/2008

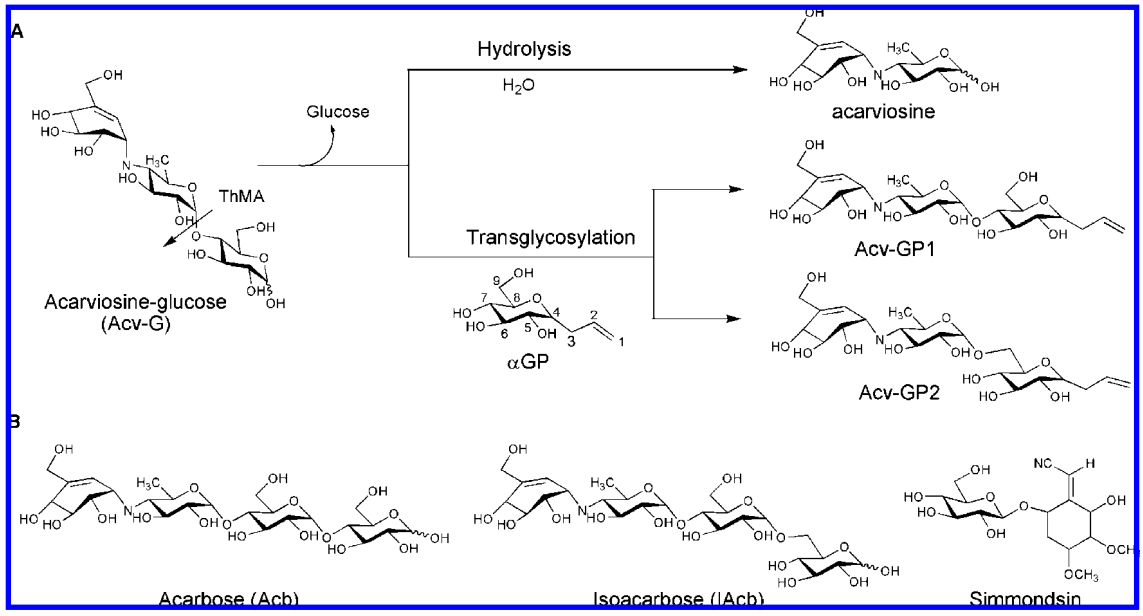

Figure 1. (**A**) Scheme of the transglycosylation reaction catalyzed by ThMA with acarbiosine-glucose and αGP. The carbons of αGP are numbered. (**B**) Chemical structures of compounds mentioned in this study: acarbose (Acb), isoacarbose (IAcb), and simmondsin.

glucose (Acv-G) and glucose, and subsequently transfer the acarviosine-glucosyl moiety to other sugar acceptors (*16–18*). Using the transglycosylation activity of MAases, novel acarviosine-glucosyl derivatives have been synthesized, and their inhibition potencies against α-glycosidases have been evaluated (*19, 20*). A maltogenic amylase from *Thermus* sp. (ThMA) has been characterized extensively in terms of its catalytic properties and mechanism using mutagenesis, kinetic analysis, and three-dimensional structure determination (*18, 21–23*). Of the catalytic functions of ThMA, hydrolysis activity of Acv-G is of particular interest because of the accompanying transferring activity of the resulting acarviosine to other sugar acceptors. Previously, we synthesized a novel compound with both antiobesity and hypoglycemic activity *in vivo* through transglycosylation of simmondsin, a food intake-reducing molecule found in the seeds of the jojoba plant (*24*).

In this article, we describe the enzymatic synthesis of novel acarviosinyl glycosides using Acv-G as a donor and a *C*-glucosyl compound, 3-α-D-glucopyranosylpropen (αGP) as an acceptor (**Figure 1A**). ThMA produced two stereoisomers containing either an α-(1→7)- or an α-(1→9)-glycosidic linkage between acarviosine and αGP. We investigated inhibition potencies against human pancreatic α-amylase (HPA) and rat intestine α-glucosidase (RIG) relative to acarbose. Conclusively, the α-(1→9)-linked transfer product showed a highly enhanced selectivity to RIG over HPA compared to acarbose.

MATERIALS AND METHODS

Reagents and Enzymes. Acarbose was extracted from Glucobay tablets and was purified through gel permeation chromatography (GPC) using a Bio-Gel P2 column (1 × 90 cm). In order to prepare Acv-G, 5% (w/v) acarbose in 50 mM sodium acetate buffer (pH 6.0) was incubated with 10 units of ThMA per milligram of acarbose for 24 h at 60 °C. The products were purified using GPC. Acarbose and Acv-G from GPC were desalted by preparative high performance liquid chromatography (HPLC, Waters, USA), and their purities were confirmed by high performance anion-exchange chromatography (HPAEC) analysis and thin layer chromatography (TLC). αGP was achieved via replacement of the trichloroimidate group of *per-O*-benzoyl-α-D-glycosyltrichloroimidate with a propenyl group using allyltrimethylsilane followed by deprotection using sodium methoxide in methanol. Detailed synthesis of αGP will be published elsewhere. Enzymes used in this study [ThMA (*18*), HPA (*13*), and RIG (*25*)] were prepared according to procedures published in the literature.

Preparation and Structural Analysis of Transfer Products. For the transglycosylation reaction, ThMA (20 U per mg of Acv-G) was used with 5% (w/v) Acv-G and 10% (w/v) αGP in 50 mM sodium acetate buffer (pH 6.0) at 50 °C. The transglycosylation reaction was monitored by TLC. After 24 h of incubation, the products were separated by descending paper chromatography on Whatman No. 3 MM chromatography paper (Whatman, Maidstone, UK), developed with isopropanol/ethyl acetate/water (3:1:1, v/v/v), and detected on the paper using the alkaline $AgNO_3$ dipping procedure (*26*). Each transfer product was eluted from the paper with deionized water and concentrated using a Speedvac (AES1010-120, SAVANT Instrument, Farmingdale, NY USA). Each compound was dissolved in water and subjected to recycling preparative HPLC (LC-910, JAI Ltd., Tokyo, Japan) equipped with a GPC column (W-251, 20 × 500 mm, JAI Ltd.). The eluent was monitored using a RI-50 refractive index detector (JAI Ltd.). Distilled water was used as an eluent at a flow rate of 3.0 mL/min. The chemical structures of the purified transfer products were determined using matrix-assisted laser desorption/ionization-time-of-flight mass spectrometry (MALDI-TOF MS) using a Voyager-DE system (Applied Biosystems, Foster City, CA, USA) and ^{13}C nuclear magnetic resonance (NMR) recorded with a JEOL LA-400 FT-NMR spectrometer (Jeol Ltd., Tokyo, Japan). α-Cyano-4-hydroxy-cinnamic acid (Cat. No. C-2620, Sigma Chemicals Co., St. Louis, MO, USA) was used as a matrix for MALDI-TOF MS.

Thin Layer Chromatography. A silica gel K5F thin layer chromatography plate (Whatman, Maidstone, UK) was activated by placing it for 30 min in an oven adjusted to 110 °C. Prepared samples were spotted on a silica gel plate and placed in a TLC chamber containing a solvent system of isopropyl alcohol, ethyl acetate, and water at a ratio of 3:1:0.4 (v/v/v). The TLC plate was developed twice at room temperature. The plate was dried thoroughly and developed by dipping into a methanol solution containing 3 g of *N*-(1-naphthyl)-ethylenediamine and 50 mL of concentrated H_2SO_4 per liter. The plate was dried and then placed in an oven set at 110 °C for 10 min; purple-black spots appeared on a white background.

HPAEC Analysis. The reaction mixture treated by ThMA was boiled for 10 min and centrifuged at 12,000 × *g* for 10 min and filtered using a membrane filter kit (0.45 μm, Millipore). The products were analyzed by HPAEC with a pulsed amperometric detector (ED40, Sunnyvale, CA, DIONEX). A CarboPac PA-1 column (0.4 × 25 cm, DIONEX) was used. A sample (200 μL) was injected and eluted with a gradient

Scheme 1

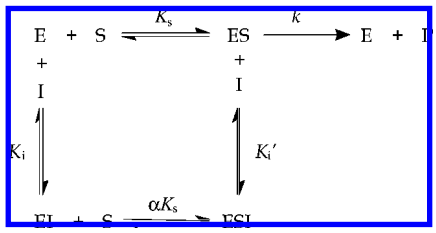

of 1 M sodium acetate (0−2 mM; 2−37 min, increased from 50 mM to 350 mM, and 37−45 min, increased from 350 mM to 850 mM) in 150 mM NaOH with a flow rate of 1 mL/min.

Enzymatic Analysis of the Structures of Transfer Products. The pure transfer products [final 0.01% (w/v)] were incubated with either isoamylase (final 1 unit/mL, Hayashibara Biochemical Laboratories Inc., Okayama, Japan) in 50 mM sodium acetate buffer (pH 5.0) at 30 °C or β-amylase (final 10 mg/mL, Cat. No. A7005, Sigma-Aldrich Co., St. Louis, MO, USA) in 50 mM sodium acetate (pH 4.5) at 50 °C. The reactions were carried out 72 h, and the reaction mixtures were analyzed by HPAEC.

Assay of Rat Intestine α-Glucosidase Activity. Assay of α-glucosidase activity was carried out at 37 °C according to the glucose oxidase/peroxidase method as described previously (*19*). The glucose-E kit (Youngdong Pharmaceutical Co., Yongin, Korea) was used according to a manual supplied by the manufacturer. Maltose (Sigma-Aldrich Co.) was used as a substrate, and the amount of glucose in the sample was calculated using a glucose calibration curve. One unit (U) of enzyme activity was defined as the amount of enzyme that splits 1 μmol of maltose in 1 min.

Assay of Human Pancreatic α-Amylase Activity. All reactions for HPA were carried out in 50 mM sodium phosphate buffer (pH 7.0) containing 6 mM NaCl at 37 °C. Soluble starch (Showa Chemical Co., Tokyo, Japan) was used as a substrate, and the amount of reducing sugars produced by HPA was measured using the copper-bicinchoninate reducing-value method (*27*).

Enzyme Inhibition Kinetics of Acarbose and Its Derivatives. The assays for RIG and HPA were conducted in the presence of the proper concentration of inhibitors. The inhibition types of the inhibitors were determined using Lineweaver−Burk plots (*28*), and kinetic parameters such as V_{max}, K_m, K_i, and K_i' were evaluated by fitting data into the following equation using the SigmaPlot program (SPSS Inc., Chicago, IL, USA):

$$v_i = \frac{V_{max} \times S}{K_m\left(1 + \frac{I}{K_i}\right) + S\left(1 + \frac{I}{K_i'}\right)} \quad (1)$$

where v_i is the initial velocity in the absence and presence of the inhibitor; S and I are the concentration of substrate and inhibitor, respectively; V_{max} is the maximum velocity, K_m is the Michaelis−Menten constant, K_i is the inhibitor constant, defined as [E][I]/[EI] in **Scheme 1**, and K_i' corresponds to the inhibition constant defined as [ES][I]/[ESI].

RESULTS AND DISCUSSION

Preparation of Transfer Products. Acarviosine is unstable and rearranges itself to form a tricyclic compound (*5*). After self-rearrangement of acarviosine, it was not detectable by the general carbohydrate visualization methods using the *N*-(1-napthyl) ethylenediamine−sulfuric acid reagent or the sulfuric acid procedure. However, we could monitor the reaction progress using the production of glucose by ThMA (**Figure 2**, lanes 3 and 4). The transglycosylation reaction yielded two transfer products (product 1 and 2) with less than 10% yields based on the TLC result. These compounds were purified homogeneously by paper chromatography and recycling preparative-HPLC (**Figure 2**, lanes 5 and 6).

Structural Analysis of Transfer Products. The purified compound 1 and 2 were analyzed by MALDI-TOF MS to determine their molecular masses. The peak appeared at *m*/*z* 530, which corresponds to the molecular mass of a sodium adduct of α-D-acarviosinylglucopyranosylpropen (Acv-αGP, calculated molecular mass = 507 Da). The mass spectrum also suggested that compound 2 is an isomer with the same molecular mass as that of compound 1. Given the regioselectivity of transglycosylation by ThMA and other MAases (*16–18*), the expected chemical structures of these compounds were either α-(1→7)-linked Acv-αGP (a compound corresponding to α-(1→4)-linked glycoside transfer products by ThMA) or α-(1→9)-linked Acv-αGP (a compound corresponding to α-(1→6)-linked glycoside transfer products by ThMA).

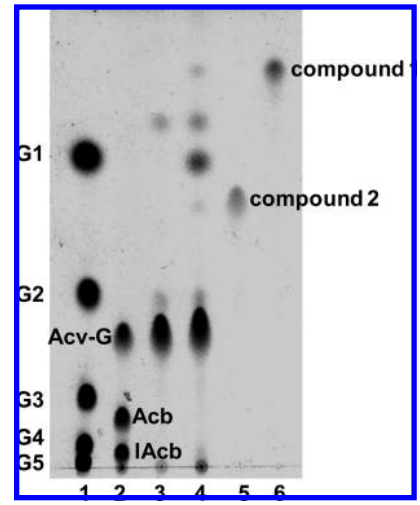

Figure 2. Thin layer chromatography analysis of the reaction catalyzed by ThMA. Lane 1: maltodextrin standards (G1-G5); lane 2: acarbose standard [Acv-G, acarbose (Acb), and isoacarbose (IAcb)]; lane 3: before reaction; lane 4: after reaction; lane 5: isolated compound 2; lane 6: isolated compound 1.

^{13}C NMR analyses of the isolated transfer products were carried out, and chemical shifts of Acv-αGPs were compared to those of αGP and Acv-G in the ^{13}C NMR spectrum (**Table 1**). The chemical shifts of Acv-G were identified using the previous studies (*20, 24*). In the case of compound 1, there was a large chemical shift from 74.1 to 79.5 ppm of C-7 of αGP (ring C in **Table 1**), indicating that the acarviosine group was linked to C-7 of αGP. From these results, the chemical structure of compound 1 was defined as α-acarviosinyl-(1→7)-3-α-D-glucopyranosylpropen (Acv-GP1). As shown in **Table 1**, there was a large chemical shift of C-9 of αGP from 61.8 to 69.6 ppm, suggesting that the acarviosine group was linked to C-9 of αGP. From these results, the chemical structure of compound 2 was determined as α-acarviosinyl-(1→9)-3-α-D-glucopyranosylpropen (Acv-GP2). The overall reaction mechanism of transglycosylation by ThMA in this study is summarized in **Figure 1A**.

In order to confirm our NMR analysis, enzymatic hydrolysis of two transfer products was carried out using β-amylase and isoamylase, and the reaction mixtures were analyzed by using HPAEC. The preliminary hydrolysis test of acarbose using these enzymes, β-amylase was able to hydrolyze acarbose, resulting in the production of acarviosine and maltose (Supporting Information). However, isoamylase, which can hydrolyze only α-(1→6)-glycosidic linkages in amylopectin or glycogen, did not hydrolyze acarbose. Acv-GP1 was hydrolyzed by only β-amylase into acarviosine and αGP, but isoamlyase did not cleave Acv-GP2 (Supporting Information). The results of HPAEC analysis, therefore, revealed that the acarviosine residue of Acv-GP1 is linked to C-7 of αGP, corresponding to C-4 of

Table 1. ^{13}C NMR Chemical Shifts of Acarbose, αGP, Acv-GP1, and Acv-GP2

				(unit: ppm)			
				Acv-GP1[c]		Acv-GP2[d]	
carbon atoms		acarbose[a]	αGP[b]	chemical shift	Δδ	chemical shift	Δδ
ring A	1	56.0		56.1	+0.1	56.0	0
	2	123.8		123.9	+0.1	123.8	0
	3	139.0		139.0	0	139.0	0
	4	71.2		70.9	+0.3	71.0	−0.2
	5	74.0		74.4	0	73.5	−0.5
	6	72.7		72.7	0	71.7	−1.0
	7	61.6		60.8	−0.8	60.4	−1.2
ring B	1	99.8		99.8	0	97.7	−2.1
	2	70.8		70.8	0	70.8	0
	3	73.0		73.0	0	72.5	−0.5
	4	65.0		65.0	0	65.2	+0.2
	5	69.6		69.7	+0.1	70.0	+0.4
	6	17.3		17.4	+0.1	17.3	0
ring C	1		118.3	117.6	−0.7	117.6	−0.7
	2		135.5	134.6	+0.1	134.6	−−0.9
	3		29.7	29.5	−0.2	28.7	−1.0
	4		73.3	73.0	−0.3	73.0	−0.3
	5		76.2	77.7	+1.5	75.6	−0.6
	6		71.1	71.2	+0.1	71.2	+0.1
	7		**74.1**	**79.5**	**+5.4**	74.2	+0.1
	8		72.0	71.8	−0.2	71.0	+1.0
	9		**61.8**	61.7	−0.1	**69.6**	**+7.8**

[a] Acarbose, ^{13}C NMR data of acarviosine residue of acarbose in this table. [b] αGP, 3-α-D-glucopyranosylpropen. [c] Acv-GP1, [d] Acv-GP2.

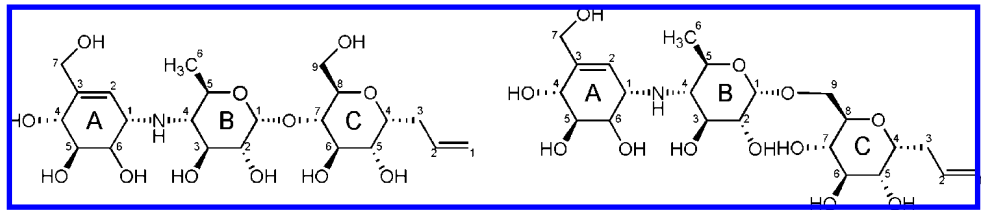

Table 2. Analysis of Inhibition against A-Amylase and A-Glucosidase by Acarbose and Transfer Products[a]

enzyme	substrate	inhibitors	type of inhibition	K_i[b] (μM)	K_i'[c] (μM)	inhibitor potency[d]
HPA[e]	starch	acarbose	mixed	2.3	5.0	1.0
		Acv-GP1	mixed	2.6	8.4	0.9
		Acv-GP2	mixed	6.7	77	0.3
RIG[f]	maltose	acarbose	competitive	0.3		1.0
		Acv-GP1	competitive	0.6		0.5
		Acv-GP2	competitive	0.1		3.0

[a] Error ranges in this table are 5−10%. [b] K_i is the inhibition constant, defined as [E][I]/[EI]. [c] K_i' is the inhibition constant, defined as [EI][S]/[ESI]. [d] Inhibitor potencies for α-glucosidase and α-amylase are calculated on the basis of assigning the value of acarbose as 1 and dividing the K_i value of acarbose by the K_i value of the inhibitor. [e] HPA, human pancreatic α-amylase. [f] RIG, rat intestine α-glucosidase.

glucose (**Figure 1**). By contrast, isoamylase only hydrolyzed Acv-GP2 into acarviosine and αGP, but Acv-GP1 was not hydrolyzed (Supporting Information). The isoamylase treatment of the transfer products allowed us to confirm that Acv-GP2 has a α-(1→9)-glycosidic linkage between acarviosine and αGP, which corresponds to the α-(1→6)-glycosidic linkage of amylopectin and glycogen.

Inhibition of Acarbose and Its Derivatives against HPA. The inhibitory activities of acarbose and two derivatives (Acv-GP1 and Acv-GP2) against HPA were investigated (**Table 2**). All inhibitors showed mixed type inhibition behaviors against HPA, and this result is consistent with our previous studies of other acarbose derivatives against porcine pancreatic α-amylase (*19, 24*). The values of K_i of acarbose, Acv-GP1, and Acv-GP2 were determined to be 2.3, 2.6, and 6.7 μM, respectively (**Table 2**). Acv-GP1, which differs from the parent molecule (Acv-G) only in the group at the anomeric center of the reducing end, where a propenyl group replaces a hydroxyl group (**Figure 1**), showed inhibition potency (0.9-fold of acarbose inhibition) very similar to that of Acv-G (1.2-fold of acarbose inhibition; from ref *19*). In contrast, the counterpart (Acv-GP2) exhibited relatively low inhibition potency (0.3-fold of acarbose inhibition).

Acarbose is rearranged by HPA, and the resulting pseudopentasaccharide is found in the active site of HPA (*13*). However, isoacarbose, whose glucose moiety at the reducing end is linked to Acv-G via an α-(1→6)-glycosidic linkage (**Figure 1B**), is resistant to the enzymatic rearrangement (*14*). Likewise, Acv-G and Acv-GP1, with inhibition potency similar to that of acarbose, would bind to HPA at subsites

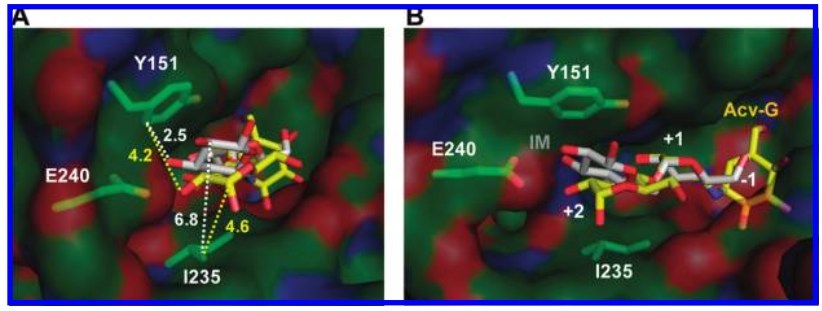

Figure 3. Electrostatic potential of the surface of HPA active site with acarviosine-glucose. Part **B** represents the model structure in **A** rotated in a counterclockwise direction by 90°. A coordinate for the structures used in this figure was 1XCW (*14*) obtained from the Protein Data Bank. Acv-G (yellow color for carbon atoms) and isomaltose (IM, gray color for carbon atoms) in the active site are presented as sticks. The ring of Acv-G bound in the +1 subsite was used as the basis for superposition with the glucose ring of IM. A coordinate for the structures of IM was obtained from isoacarbose bound in HPA [PDB file 1XCX (*14*)]. The distances between the amino acid residues of HPA and Acv-G are indicated with yellow dashed lines in **A**. The distances between amino acid residues of HPA and IM are represented as white dashed lines in **A**. The subsites −1 through +2 of HPA are indicated in the **B**. The figure was made using PyMol v.0.99.

−1 through +2 without the enzymatic rearrangement. Acv-GP2, which is also expected to bind to HPA without rearrangement, showed lower inhibition potency than other α-(1→4)-linked pseudotrisaccharides (Acv-G and Acv-GP1). Therefore, these inhibition patterns of αGPs are consistent with the investigation of acarviosine-α-(1→6)-simmondsin (Acv-6-Sim) by Baek et al. (*24*) and suggest that subsites +1 and +2 of HPA are oriented for the binding of linear α-(1→4)-linked maltooligosaccharides or their derivatives rather than α-(1→6)-linked counterparts.

To investigate the specificity and mechanism of inhibition by acarviosine derivatives, a model structure of HPA with an isomaltose (IM) bound in subsites +1 and +2 was established using the enzyme−inhibitor complex of HPA with Acv-G (*14*). Upon using the ring of Acv-G (yellow) bound in the +1 subsite as the basis for superposition with the nonreducing end-glucose ring of IM (gray), it is clear that O-3′ of the glucose residue of IM in the +2 subsite would clash with Tyr151 (2.5 Å away from O-3 of the glucose residue of IM, **Figure 3**). In addition, hydrophobic interaction between Ile235 of HPA and the glucose ring at the reducing end of Acv-G would be removed because of the distortion of the sugar chain by the α-(1→6)-glycosidic linkages compared to Acv-G. Upon binding of Acv-GP2, the αGP residue is expected to locate at the position of the reducing end of IM. Therefore, the architecture of the active site of HPA around the +2 subsite interacting with the glucose residue of Acv-G may not allow proper binding of the αGP residue of Acv-GP2 in the +2 subsite of HPA.

Inhibition of Acarbose and Its Derivatives against RIG. Next, we explored the inhibition potencies of the inhibitors against RIG. Lineweaver−Burk plots for inhibition against RIG clearly show that their inhibition modes are competitive. As in the case of HPA, Acv-GP1 showed inhibition potency against RIG similar to that of Acv-G; the K_i value of Acv-GP1 was 0.6 μM, corresponding to 0.5-fold inhibition by acarbose (**Table 2**). Acv-G showed inhibition 0.4-fold of that of acarbose (*19*). Interestingly, a value of 0.1 μM was determined for the K_i value of Acv-GP2, which translates to 6-fold and 3-fold enhanced inhibition potency relative to that of Acv-GP1 and acarbose, respectively (**Table 2**). This result suggests that α-(1→9)-linked αGP of Acv-GP2 may lead to a tighter binding of Acv-GP2 to the active site of RIG. Overall, the selectivity of Acv-GP2 against α-glucosidase over α-amylase is enhanced 10-fold relative to that of acarbose.

Very recently, the three-dimensional structure of the N-terminal catalytic subunit of human intestine maltase-glucoamylase (NtMGAM) was solved (*29*). In the complex structure of the human enzyme with acarbose, acarviosine clearly binds in the −1 and +1 subsites, but there was no evidence for the presence of +2 and +3 subsites for binding of the maltose residue, which is linked via linear α-(1→4)-glycosidic linkages (*29*). The 3-D structural information has not been released yet, but we are expecting that the structure of RIG and the binding mode of the inhibitor in the active site of RIG may be similar to those of NtMGAM. Therefore, the structural information on NtMGAM and the inhibition kinetics of Acv-GP2 in this study allow us to anticipate that the acarviosine residue of Acv-GP2 binds in the −1 and +1 subsites of RIG, and additional interactions would be possible between the enzyme and αGP of Acv-GP2 that were not present in the complex structure, NtMGAM:acarbose. However, Acv-6-Sim, which is another α-(1→6)-linked acarviosinyl glycoside, has worse inhibition potency than that of Acv-G (*24*). Probably, steric hindrances caused by a β-linked bulky 2-(cyanomethylene)-3-hydroxy-4,5-dimethoxycyclohexyl group in simmondsin (see **Figure 1B**) are responsible for weakening the affinity of Acv-6-Sim to RIG. The smaller and α-glycosidic-linked propenyl group in αGP would reduce such steric hindrances in the Acv-6-Sim case.

CONCLUSIONS

Here, we synthesized two novel Acv-G derivatives through enzymatic transglycosylation catalyzed by ThMA using Acv-G as a donor and αGP as an acceptor. Of these products, Acv-GP2 with a structure corresponding to the α-(1→6)-linked transfer product showed a 10-fold enhanced selectivity toward α-glucosidase over α-amylase compared to acarbose. On the basis of the model structure of the HPA−inhibitor complex, Acv-GP2 seems to be unfitted into the active site of HPA, resulting in a lower inhibition potency than those of acarbose and Acv-GP1. A higher α-glucosidase inhibition potency of Acv-GP2 than those of acarbose and Acv-GP1 implies that additional interaction would be generated by the binding of Acv-GP2 in the active site of RIG. Conclusively, this α-glucosidase-specific inhibition by Acv-GP2 would not only allow sufficient hydrolysis of carbohydrate in the diet by α-amylases but also decrease blood glucose by strong inhibition against α-glucosidases.

ABBREVIATIONS USED

ThMA, maltogenic amylase from *Thermus* sp.; MAases, maltogenic amylases; HPA, human pancreatic α-amylase; RIG, rat intestine α-glucosidase; GPC, gel permeation chromatography; HPLC, high performance liquid chromatography; HPAEC, high performance anion-exchange chromatography; TLC, thin layer chromatography; MALDI-TOF MS, matrix-assisted laser desorption/ionization-time-of-flight mass spectrometry; NMR, nuclear magnetic resonance; Acv-G, acavosine-glucose; αGP, 3-α-D-glucopyranosylpropen; Acv-αGP, α-D-acarviosinylglucopyranosylpropen; Acv-6-Sim, acarviosine-α-(1→6)-simmondsin; Acv-GP1, α-acarviosinyl-(1→7)-3-α-D-glucopyranosylpropen; Acv-GP2, α-acarviosinyl-(1→9)-3-α-D-glucopyranosylpropen; IM, isomaltose; NtMGAM, N-terminal catalytic subunit of human intestine maltase-glucoamylase.

Supporting Information Available: HPAED chromatograms of the reaction mixtures of acarbose by *β*-amylase and isoamylase, HPAED chromatograms of the reaction mixtures of Acv-PG1 by *β*-amylase and isoamylase, HPAED chromatograms of the reaction mixtures of Acv-GP2 by α-amylase and isoamylase, Lineweaver−Burk plots of the reactions of human pancreatic α-amylase inhibition in the presence of acarbose, Acv-GP1, and Acv-GP2, and Lineweaver−Burk plots of the reactions of rat intestinal α-glucosidase inhibition in the presence of acarbose, Acv-GP1, and Acv-GP2. This material is available free of charge via the Internet at http://pubs.acs.org.

LITERATURE CITED

(1) Asano, N.; Nash, R. J.; Molyneux, R. J.; Fleet, G. W. J. Sugar-mimic glycosidase inhibitors: natural occurrence, biological activity and prospects for therapeutic application. *Tetrahedron: Asymmetry* **2000**, *11*, 1645–1680.

(2) Bols, M. 1-aza sugars, apparent transition state analogues of equatorial glycoside formation/cleavage. *Acc. Chem. Res.* **1998**, *31*, 1–8.

(3) Winchester, B.; Fleet, G. W. J. Amino-sugar glycosidase inhibitors: Versatile tools for glycobiologists. *Glycobiology* **1992**, *2*, 199–210.

(4) Bischoff, H. The mechanism of α-glucosidase inhibition in the management of diabetes. *Clin. Invest. Med.* **1995**, *18*, 303–311.

(5) Junge, B.; Boshagen, H.; Stoltefu, J.; Müller, L. *Derivatives of Acarbose and Their Inhibitory Effects on* α*-Glucosidase*; Verlag Chemie: Weinheim, Germany, 1981.

(6) Truscheit, E.; Frommer, W.; Junge, B.; Müller, L.; Schmidt, D. D.; Wingender, W. Chemistry and biochemistry of microbial α-glucosidase inhibitors. *Angrew. Chem., Int. Ed. Engl.* **1981**, *20*, 774–761.

(7) Chiasson, J. L.; Josse, R. G.; Gomis, R.; Hanefeld, M.; Karasik, A.; Laakso, M. Acarbose for prevention of type 2 diabetes mellitus: the STOPNIDDM randomised trial. *Lancet* **2002**, *359*, 2072–2077.

(8) Balfour JA, M. D. Acarbose. An update of its pharmacology and therapeutic use in diabetes mellitus. *Drugs* **1993**, *46*, 1025–1054.

(9) Brzozowski, A. M.; Davies, G. J. Structure of the *Aspergillus oryzae* α-amylase complexed with the inhibitor acarbose at 2.0 Å resolution. *Biochemistry* **1997**, *36*, 10837–10845.

(10) Strokopytov, B.; Penninga, D.; Rozeboom, H. J.; Kalk, K. H.; Dijkhuizen, L.; Dijkstra, B. W. X-ray structure of cyclodextrin glycosyltransferase complexed with acarbose. Implications for the catalytic mechanism of glycosidases. *Biochemistry* **1997**, *34*, 2234–2240.

(11) Gilles, C.; Astier, J. P.; Marchis-Mouren, G.; Cambillau, C.; Payan, F. Crystal structure of pig pancreatic α-amylase isoenzyme II, in complex with the carbohydrate inhibitor acarbose. *Eur. J. Biochem.* **1996**, *238*, 561–569.

(12) Qian, M. N. V.; Bonicel, J.; Bischoff, H.; Henrissat, B.; Payan, F. Enzyme-catalyzed condensation reaction in a mammalian α-amylase. High-resolution structural analysis of an enzyme-inhibitor complex. *Biochemistry* **2001**, *40*, 7700–7709.

(13) Brayer, G. D.; Sidhu, G.; Maurus, R.; Rydberg, E. H.; Braun, C.; Wang, Y.; Nguyen, N. T.; Overall, C. M.; Withers, S. G. Subsite mapping of the human pancreatic α-amylase active site through structural, kinetic, and mutagenesis techniques. *Biochemistry* **2000**, *39*, 4778–4791.

(14) Li, C.; Begum, A.; Numao, S.; Park, K. H.; Withers, S. G.; Brayer, G. D. Acarbose rearrangement mechanism by the kinetic and structural analysis of human pancreatic α-amylase in complex with analogues and their elongated counterparts. *Biochemistry* **2005**, *44*, 3347–4457.

(15) Numao, S.; Damager, I.; Li, C.; Wrodnigg, T. M.; Begum, A.; Overall, C. M.; Brayer, G. D.; Withers, S. G. In situ extension as an approach for identifying novel α-amylase inhibitors. *J. Biol. Chem.* **2004**, *279*, 48282–48291.

(16) Park, K. H.; Kim, T. J.; Cheong, T. K.; Kim, J. W.; Oh, B. H.; Svensson, B. Structure, specificity and function of cyclomaltodextrinase, a multispecific enzyme of the α-amylase family. *Biochim. Biophys. Acta* **2000**, *1478*, 165–185.

(17) Cha, H. J.; Yoon, H. G.; Kim, Y. W.; Lee, H. S.; Kim, J. W.; Kweon, K. S.; Oh, B. H.; Park, K. H. Molecular and enzymatic characterization of a maltogenic amylase that hydrolyzes and transglycosylates acarbose. *Eur. J. Biochem.* **1998**, *253*, 251–262.

(18) Kim, T. J.; Kim, M. J.; Kim, B. C.; Kim, J. C.; Cheong, T. K.; Kim, J. W.; Park, K. H. Modes of action of acarbose hydrolysis and transglycosylation catalyzed by a thermostable maltogenic amylase, the gene for which was cloned from a *Thermus* strain. *Appl. Environ. Microbiol.* **1999**, *65*, 1644–1651.

(19) Kim, M. J.; Lee, S. B.; Lee, H. S.; Baek, J. S.; Kim, D.; Moon, T. W.; Robyt, J. F.; Park, K. H. Comparative study of the inhibition of α-glucosidase, α-amylase, and cyclodextrin glucanosyltransferase by acarbose, isoacarbose, and acarviosine-glucose. *Arch. Biochem. Biophys.* **1999**, *317*, 277–283.

(20) Bae, H. K.; Lee, S. B.; Park, C. S.; Shim, J. H.; Lee, H. Y.; Kim, M. J.; Baek, J. S.; Roh, H. J.; Choi, J. H.; Choe, E. O.; Ahn, D. U.; Park, K. H. Modification of ascorbic acid using transglycosylation activity of *Bacillus stearothermophilus* maltogenic amylase to enhance its oxidative stability. *J. Agric. Food Chem.* **2002**, *50* (11), 3309–3326.

(21) Kim, J. S.; Cha, S. S.; Kim, H. J.; Kim, T. J.; Ha, N. C.; Oh, S. T.; Cho, H. S.; Cho, M. J.; Kim, M. J.; Lee, H. S.; Kim, J. W.; Choi, K. Y.; Park, K. H.; Oh, B. H. Crystal structure of a maltogenic amylase provides insights into a catalytic versatility. *J. Biol. Chem.* **1999**, *274*, 26279–26286.

(22) Kim, T. J.; Park, C. S.; Cho, H. Y.; Cha, S. S.; Kim, J. S.; Lee, S. B.; Moon, T. W.; Kim, J. W.; Oh, B. H.; Park, K. H. Role of the glutamate 332 residue in the transglycosylation activity of *Thermus* maltogenic amylase. *Biochemistry* **2000**, *39*, 6773–6780.

(23) Kim, T. J.; Nguyen, V. D.; Lee, H. S.; Kim, M. J.; Cho, H. Y.; Kim, Y. W.; Moon, T. W.; Park, C. S.; Kim, J. W.; Oh, B. H.; Lee, S. B.; Svensson, B.; Park, K. H. Modulation of the multisubstrate specificity of *Thermus* maltogenic amylase by truncation of the N-terminal domain and by a salt-induced shift of the monomer/dimer equilibrium. *Biochemistry* **2001**, *40*, 14182–14190.

(24) Baek, J. S.; Kim, H. Y.; Abbott, T. P.; Moon, T. W.; Lee, S. B.; Park, C. S.; Park, K. H. Acarviosine-simmondsin, a novel compound obtained from acarviosine-glucose and simmondsin by *Thermus* maltogenic amylase and its in vivo effect on food intake and hyperglycemia. *Biosci. Biotechnol. Biochem.* **2003**, *67*, 532–539.

(25) Rhinehart, B. L.; Robinson, K. M.; Liu, P. S.; Payne, A. J.; Wheatley, M. E.; Wagener, S. R. Inhibition of intestinal disaccharidases and suppression of blood glucose by a new α-gluco-

hydrolase inhibitor. *J. Pharmacol. Exp. Ther.* **1987**, *241*, 915–920.

(26) Han, N. S.; Robyt, J. F. Separation and detection of sugars and alditols on thin layer chromatograms. *Carbohydr. Res.* **1998**, *313*, 135–137.

(27) Fox, J. D.; Robyt, J. F. Miniaturization of three carbohydrate analyses using a microsample plate reader. *Anal. Bbiochem.* **1991**, *195*, 93–96.

(28) Segel, I. H., *Simple Inhibition Systems in Enzyme Kinetics: Behavior and Analysis of Rapid Equilibrium and Steady-State Enzyme System*; Wiley: New York, 1975..

(29) Sim, L.; Quezada-Calvillo, R.; Sterchi, E. E.; Nichols, B. L.; Rose, D. R. Human intestinal maltase-glucoamylase: Crystal structure of the N-terminal catalytic subunit and basis of inhibition and substrate specificity. *J. Mol. Biol.* **2008**, *375*, 782–792.

Received for review December 16, 2007. Revised manuscript received March 17, 2008. Accepted April 24, 2008. This work was supported by a grant from the Korea Health 21 R&D project, Ministry of Health and Welfare, Republic of Korea (AD050376).

JF703655K